MICROSTRUCTURAL EFFECTS ON ADIABATIC SHEAR BAND FORMATION

S. Osovski[1], D. Rittel[1*], P. Landau[2] and A. Venkert[2]

[1] Faculty of Mechanical Engineering, Technion, 32000 Haifa, Israel

[2] Department of Physics, NRCN, Beer-Sheva, 84190, Israel

Dynamic recrystallization (DRX), driven by the dynamic stored energy of cold work, promotes shear localization. However, the influence of twinning remains to be investigated. We consider two model materials under impact, pure Titanium and a Ti6Al4V alloy, for which the extent of twinning and DRX differs vastly. A grain-scale finite element model shows that twinning delays DRX and consequently strain localization. Moreover, the calculated temperature elevations (local and global) remain very modest until the onset of failure.

Keywords: shear bands, micromechanical modeling, twinning, dynamic recrystallization, transmission electron microscopy (TEM)

(*) Corresponding author: merittel@technion.ac.il

A major dynamic deformation and failure mechanism of crystalline solids consists of abrupt localization of the plastic deformation into narrow zones, referred to as adiabatic shear bands (ASB) [1]. Zener and Hollomon [2] proposed that the inherent temperature rise causes material softening, which may overcome the strain hardening effect, ultimately leading to strain localization. While this point of view regarding the initiation stage of localization is broadly accepted on physical [3] and mathematical [4] grounds, it appears that for most materials which exhibit dynamic localization, the temperature rise *prior to* the loss of load-bearing capacity is quite small (see e.g. [5, 6]), and apparently insufficient to significantly soften the uniformly deforming material. Alternatively, Rittel et al. [7] proposed that the dynamic stored energy of cold work [8], namely the part of the energy that is not dissipated into heat [9, 10], causes microstructural re-arrangements whose most obvious manifestation is the formation of new nano-sized grains by dynamic recrystallization (DRX, [11, 12]). Rittel et al. [13] also showed that DRX actually precedes shear localization instead of being its outcome as commonly believed. These authors proposed that the dynamically recrystallized grains cause local softening of the surrounding hardened matrix material, thereby providing the necessary perturbation whose growth is the shear band itself. Concerning nanograins, Ramesh et al.[14] showed that pure iron, which does not tend to localize when the grain size is coarse, will actually undergo localization if the grain size is reduced to a few nanometers, analogous to dynamically recrystallized grains. Additional information on the lack of strain-hardening of nanograined materials can be found in Brechet et al.[15], and in Ramesh et Al. [16] for Titanium. However, another major deformation mechanism, namely *twinning*, is likely to operate in many metals and alloys, and one may wonder about its specific role in the process of strain localization. Here, one should note the important observation of Padilla et al [17] who showed that, contrary to dislocations activity,

twinning does not store significant amounts of energy, even if the twinning material can be observed to strain-harden (see also Bever et al.[8]). In this research we demonstrate how the lack of energy storage by twins may act as a retarding factor for the formation of DRX, thereby reducing their susceptibility to shear localization.

Two model materials are compared in this study. The first is a Ti6Al4V, which was found to recrystallize dynamically roughly at mid-range of the strain to failure, with a small amount of twins [13]. The second is commercially pure α-Titanium, in the annealed condition with average grain size of $\sim 100\mu m$. This material was selected to demonstrate the effect of twinning on DRX formation, and subsequently shear localization. Dynamic experiments were carried out on Titanium shear compression specimens (SCS) [18, 19]. The SCS consists of a cylinder with two opposing grooves in 45^o degrees to the longitudinal direction, with a $10mm$ diameter, $2.5mm$ gauge thickness, and $2mm$ gage width. This unique geometry enforces a state of dominant shear in the gauge section of the specimen [19], while a mild stress concentration exists in the fillets of the grooves, thus dictating the locus for shear band formation. The dynamic experiments where carried out using a split Hopkinson pressure bar (Kolsky) apparatus [20] at a strain rate of $\dot{\varepsilon} \approx 7000\ \text{sec}^{-1}$. The specimens were deformed to controlled levels of (normalized) strain, ranging from $0.3\varepsilon_f$ to complete failure, ε_f being the strain to failure. The maximum imparted strain was controlled by the use of Maraging steel stop rings. Transmission electron microscope (TEM) specimens were prepared from the fillet area for each strain level, to study the microstructural evolution leading to catastrophic failure (Figure 1a). As for Ti6Al4V [13], dynamically recrystallized grains were observed in pure Titanium prior to failure. However, while in the Ti6Al4V alloy (which hardly forms twins) DRX was readily observed at strains as low as $\varepsilon = 0.45\varepsilon_f$, no dynamically recrystallized grains were

observed in the pure Titanium up to a strain of $\varepsilon = 0.9\varepsilon_f$. Here, the observed microstructure consists of areas exhibiting massive twinning activity, along with regions showing a high density of dislocations. Beyond $\varepsilon = 0.9\varepsilon_f$, the microstructure comprises distinct islands in which *either* dynamically recrystallized grains and a high density of dislocations were observed (Fig 1b), *or* areas with dense microtwins (Fig 1c). *No DRX was observed in areas that exhibited microtwins and vice versa.* Keeping in mind that twins do not store energy, and thus cannot supply the driving force for the recrystallization process, the delayed appearance of DRX in pure Titanium with respect to Ti6Al4V leads to the conclusion that *twinning mediated plasticity acts as a delaying factor for the appearance of shear bands*.

In order to model the interplay between slip and twinning, a numerical micro-mechanical model was formulated. In addition to the continuum mechanics formulation, this model comprises two internal physical variables, namely the twins and DRX volume fractions. Since the finite element method (FEM) was used to solve the equations of motion, the typical finite element size ($100\mu m$) was set to represent a single material grain, without detailing its plastic deformation mechanisms from crystal plasticity concepts [21] (i.e., grain-scale simulations). The hardening and evolution equations for the internal variables were derived based on the following assumption: Three deformation micro-mechanisms are assumed to operate, namely twinning, slip, and a third mechanism through which the dynamically recrystallized areas deform in an ideally plastic mode. The model takes into account the main physical features of these mechanisms in terms of contribution to the global hardening and energy storage. At the beginning of the deformation process, the material deforms by both twinning and slip. The growing density of twins contributes to both the hardening and total plastic strain increment. The twin contribution to hardening is interpreted as barriers to dislocation motion, in the form of a

Hall-Petch like term (Remy [22]). The continuing dislocations' activity is described by a parabolic hardening law. The strain increment associated with twinning is considered to be a fully dissipative process, and so the relative volume which does not undergoes twinning is the sole contributor to energy storage. Once the stored energy in an element has reached a critical value, the element is assumed to undergo dynamic recrystallization, leading to the emergence of the third deformation mechanism. At this point the constitutive behavior of the element is changed since the volume fraction of twins is assumed to stop growing, and the fraction of material which undergoes slip is being progressively replaced by a DRX mediated plasticity mechanism. The dynamically recrystallized phase is assumed to behave as ideally plastic [15, 16], thus acting as a soft enclave in the continuously hardening surrounding matrix. Based on the above, the viscoplastic response of the material is given by Equation set (1):

$$\dot{\varepsilon}^p = \dot{\varepsilon}^0 \left[\frac{\sigma_{flow}}{g\left(\varepsilon^p\right)} \right]^n \qquad (1a)$$

$$g\left(\varepsilon^p\right) = \left(1 - f_{drx}\right)\sigma_y^0 + f_{drx}\sigma^{drx} + \left(1 - f_{drx} - f_{twins}\right)R\left(x, \varepsilon_m\right) \qquad (1b)$$

$$R\left(x, \varepsilon_m\right) = K_t\left(\frac{1}{x}\right) + K_d\left(\varepsilon_m\right)^m \qquad (1c)$$

The flow stress σ_{flow} is formulated as a rule of mixture over the three micro-mechanism assumed to take place (Equation (1a)). The first term in Equation (1b) refers to the yield stress of the coarse-grained Titanium ($\sigma_y^0 = 540\left[MPa\right]$), while σ^{drx} in the second term is the flow stress at which DRX originates (based on energy considerations). From thereon, the material no longer strain-hardens, each of the above mentioned stresses is thus multiplied by its relative volume fraction ($f_{drx,}\ f_{twins}$). The third term in Equation (1b) is an isotropic hardening term, $R\left(x, \varepsilon_m\right)$, which consists of two parts (Equation (1c)). The first term in this equation is a Hall-Petch like

term, when K_t $\left(0.0012\left[MPam\right]\right)$ is a hardening constant and x is the average distance between twins given by $x=2t\left(1-f_{twins}\right)/f_{twins}$ with t being the average twin width $\left(1\left[\mu m\right]\right)$, measured using optical microscopy. Note that the Hall-Petch exponent is taken as 1 instead of the usual square root, implying that dislocation pile-ups against a twin boundary cannot activate a dislocation source [22].

The second hardening term in Equation (1c) is taken as a parabolic hardening law to describe the dislocation activity during deformation with $K_d\left(230\left[MPa\right]\right), m\left(0.25\right)$ being the hardening constants, and ε_m being the strain in the non-twinned regions. Both K_t and K_d, as well as m, were calibrated by fitting the stress-strain curve to the experimental one. Finally, the rate dependence of the flow stress is given by the Equation (1a). Here, $\dot{\varepsilon}^p$ is the plastic strain rate, ε^p being the plastic strain and $n\left(0.0538\right)$ is a rate-sensitivity constant, obtained by fitting a linear line to a logarithmic plot of the stress at $\varepsilon=0.15$ vs. the strain rate as measured in the range of $\dot{\varepsilon}=1000-8500\left[\sec^{-1}\right]$, and $\dot{\varepsilon}^0\left(1000\left[\sec^{-1}\right]\right)$ is a reference strain rate. The total plastic strain is divided into strain coming from an increase in twin volume fraction, and strain arising from dislocation motion and dynamic recrystallization. The total plastic strain increment is thus given by:

$$d\varepsilon_p=\left(1-f_{twins}\right)d\varepsilon_m+\varepsilon_T df_{twins} \qquad (2)$$

When $\varepsilon_T\left(0.174\right)$ is the strain due to twinning which is taken to be the shear strain of the active twinning system divided by the Taylor factor [23]. The evolution equation of the twin volume fraction (Equation (3a)), is taken to be a function of the plastic strain alone, were a, b and N are fitted to reproduce the experimentally observed values of average number of twins per grain at

different strains. Since no quantitative experimental data exists as to the relative volume fraction of dynamically recrystallized grains evolution, the volume fraction of this phase (equation (3b)) was assumed to be describe by the Johnson-Mehl-Avrami-Kolmogorov equation [24] as a function of the stored energy of cold work (U).

$$f_{twins} = \begin{cases} \frac{1}{N}\left[\arctan\left(2\pi a\varepsilon_p - 2\pi b\right) - \arctan\left(-2\pi b\right)\right] & ;\ U < U_{drx} \\ Const. & U \geq U_{drx} \end{cases} \qquad (3a)$$

$$f_{drx} = \begin{cases} 0 & ;\ U < U_{drx} \\ 1 - \exp\left(-k_{drx}\left(\frac{U - U_{drx}}{U_{drx}}\right)^{n_{drx}}\right) & U \geq U_{drx} \end{cases} \qquad (3b)$$

With $U_{drx}\left(98\left[MPa/m^3\right]\right)$ - the threshold energy for the beginning of the recrystallization process determined from the experimental value of total mechanical work up to the first observation of the dynamically recrystallized grains, multiplied by the Quinney-Taylor coefficient [10], as measured by Rosakis et al. [25]. Here, $k_{drx}\left(0.7\right), n_{drx}\left(2.8\right)$ are rate constants, which were calibrated by fitting the calculated stress-strain curve to the experimental curve. As seen in Equation (3a), it was assumed that once an element starts to form dynamically recrystallized grains (i.e. $U > U_{drx}$), the volume fraction of twins stops growing. Since both twin and DRX do not store any significant amount of energy, it was assumed that the stored energy comes *solely* from the phase which undergoes slip, and is given by Equation (4):

$$U = (1-\beta)\int_0^{\varepsilon_m} \sigma_{flow} d\varepsilon_m \qquad (4)$$

With $\beta = 0.6$ being the Quinney -Taylor coefficient [10] applied only to the slipped material. The amount of energy dissipated into heat is then easily calculated using the first law of thermodynamics and thus the temperature rise can be calculated by assuming adiabatic

conditions using equation set (5) where $\rho = 4500\left[Kg / m^3 \right]$ is the density and

C_p=5.28$\left[J/KgK\right]$is the specific heat capacity.

$$\left.\begin{aligned} W - U &= \int \sigma_{flow} d\varepsilon^p - U = Q \\ \Delta T &= \frac{Q}{\rho C_p} \end{aligned}\right\} \qquad (5)$$

Numerical (FEM) simulations of the compression of a SCS specimen were carried out using ABAQUS\Explicit (ver.6.92) solver, into which the above model was implemented using the numerical scheme suggested by Anand et Al. [26]. To simulate the heterogeneity arising from the different grain orientations, each grain was assigned a slightly different Taylor factor [23] from a random uniform distribution. The measured velocities were applied on the specimen faces as a boundary condition. It is important to note that no failure criterion was implemented into the simulation, so that each subsequent reference to the failure is strictly experimental, namely failure in the numerical simulation takes place at the experimentally measured failure strain.

Fig. 2 shows the build-up of the average volume fraction of the dynamically recrystallized phase as a function of the average plastic strain in the gauge section. Up to failure, the amount of DRX is relatively small, in agreement with the electron micrographs (Fig. 1). By contrast, the evolution of the twins' volume fraction (Fig. 2) reveals a massive buildup from the very onset of plastic deformation. This result reflects the input conditions assumed in the model, in the sense that the evolution of twinning with plastic strain and the critical energy for DRX were both taken from experimental observations and considerations. The mechanical influence of the dynamically recrystallized grains is illustrated by considering the distribution of strain rates in the vicinity of a dynamically recrystallized grain (Fig. 3a). Here, one can appreciate the radius of influence of this grain, over which the strain-rate is noticeably amplified with respect to the

calculated average strain-rate in the deformed gauge. It is noted that the first shell of elements surrounding the dynamically recrystallized grain undergoes significant structural strain-softening. In parallel to the observed structural strain-softening, the maximum local temperature that develops in the deformed gauge was calculated. Here, it should be emphasized that, instead of calculating a global temperature change based on continuum considerations for the whole sheared gage (e.g. using Equation (5) with a constant and unique Taylor-Quinney factor), the temperature change is calculated on an element-basis with a Taylor-Quinney coefficient that varies according to the grain-size microstructural evolution. Fig 3b shows the local maximum temperature as a function of the plastic strain, revealing that the maximum calculated temperature at macroscopic failure does not exceed 0.3Tm. This result is in accord with previous average quantitative measurements, so that the global thermal softening influence, or even the eventual formation of "hot-spots" as triggers for instability, seems to be quite negligible, at the benefit of the observed microstructural softening mechanism. The spatial evolution of the dynamically recrystallized phase (which initially concentrates in the fillet areas of the specimen due to stress concentration) is shown in Fig. 4. Discontinuous islands of DRX originate in this area, and as strain increases, the number and the size of the islands both grow until formation of a continuous band of the recrystallized phase. Continuity of the band is completed close to the observed failure strain, thus reinforcing the relationship between DRX and localized shear failure. The localization is understood here as a continuous band of material in which the local strain-rate exceeds significantly the average strain-rate.

This study addresses twinning-related aspects of shear localization that were not previously considered. Given that dynamic recrystallization promotes shear localization [13], the systematic comparison of two materials shows that twinning, present in pure Ti but absent in Ti6Al4V, will

significantly postpone the formation of DRX enclaves, which in turn confers Ti its superior resistance to adiabatic shear failure. From an energy storage point of view [7, 17], twinning is an active source for dissipation which therefore delays DRX formation. The observed kinetics of DRX and twinning were modeled numerically at the grain-scale. The calculated energy balance allowed for a local estimation of the temperature rise which overall remains quite modest, a point that emphasizes microstructural factors at the expense of thermal softening at the initiation stage of the localization process. New insight on microstructural softening related to DRX was obtained by considering local variations of the strain-rate in the vicinity of enclaves of DRX. Finally, kinetics of growth of those enclaves, which cannot be assessed experimentally, was visualized numerically, indicating what might remind of percolation effects. The results of this study indicate that, in order to reduce the susceptibility of a material to dynamic shear failure, care should be taken to ensure a reduced capacity for storage of dynamic strain energy leading to recrystallization. In that respect, stacking-fault energy considerations that relate to twin formation and energy storage, might be an important parameter in the design of shear localization resistant material systems.

Acknowledgements

The authors thank Prof. A. Needleman and Dr. E. Bouchbinder for helpful discussions. The support of Israel Science Foundation (grant 2011362) is gratefully acknowledged.

REFERENCES

[1] H. Tresca, Annales du Conservatoire des Arts et Métiers, 4 (1879).

[2] C. Zener, J.H. Hollomon, J. Applied Phys., 15 (1944) 22-32.

[3] Y. Bai, B. Dodd, Shear Localization: Occurrence, Theories, and Applications, Pergamon Press, Oxford, UK, 1992.

[4] T. Wright, The Physics and Mathematics of Adiabatic Shear Bands, Cambridge University Press, Cambridge, 2002.

[5] D. Rittel, Z.G. Wang, Mechanics of Materials, 40 (2008) 629-635.

[6] A. Marchand, J. Duffy, J. Mech. Phys. Solids, 36 (1988) 251-283.

[7] D. Rittel, Z.G. Wang, M. Merzer, Physical Review Letters, 96 (2006) 075502.

[8] M. Bever, D. Holt, A. Titchener, The Stored Energy of Cold Work, Pergamon Press, London, 1973.

[9] W.S. Farren, G.I. Taylor, Proc. R. Soc., A107 (1925) 422-451.

[10] G.I. Taylor, H. Quinney, Proc. Royal Soc. London, 143 (1934) 307-326.

[11] U. Andrade, M. Meyers, C. AH, Scripta Metall. and Mater., 30 (1994) 933-938.

[12] M.A. Meyers, J.C. LaSalvia, V.F. Nesterenko, Y.J. Chen, B.K. Kad, in: T.R. McNelley (Ed.) The Third International Conference on Recrystallization and Related Phenomena, 1996, pp. 279-286.

[13] D. Rittel, P. Landau, A. Venkert, Physical Review Letters, 101 (2008) 165501.

[14] Q. Wei, D. Jia, K.T. Ramesh, E. Ma, Applied Physics Letters, 81 (2002) 1240-1242.

[15] O. Bouaziz, Y. Bréchet, Y. Estrin, J.D. Embury, Scripta Materialia, 63 (2010) 477-479.

[16] D. Jia, M. Wang, K.T. Ramesh, T. Zhu, R.Z. Valiev, Applied Physics Letters, 79 (2001) 611-613.

[17] H.A. Padilla, C.D. Smith, J. Lambros, A.J. Beaudoin, I.M. Robertson, Metallurgical and Material Transactions A, 38A (2007) 2916-2927

[18] A. Dorogoy, D. Rittel, Exp. Mech., 45 (2005) 167-177.

[19] A. Dorogoy, D. Rittel, Exp. Mech., 45 (2005) 178-185.

[20] H. Kolsky, Proc. Phys. Soc. London, 62-B (1949) 676-700.

[21] F. Roters, P. Eisenlohr, L. Hantcherli, D.D. Tjahjanto, R. Bieler, D. Raabe, Acta Materialia, 58 (2010) 1152-1211.

[22] L. Remy, Acta Metallurgica, 26 (1978) 443-451.

[23] G.I. Taylor, Journal of the Institute of Metals, LXII (1938) 307-324.

[24] M. Avrami, Journal of Chemical Physics, 7 (1939) 1103-1112.

[25] G. Ravichandran, A.J. Rosakis, J. Hodowany, P. Rosakis, Physics, (2002).

[26] A.M. Lush, G. Weber, L. Anand, International Journal of Plasticity, 5 (1989) 521-549.

[27] P. Landau, A. Venkert, D. Rittel, Metallurgical and Material Transactions A, 41 (2010) 389-396.

Figure Legends

Figure 1. TEM micrographs showing the microstructure of Titanium SCS specimens deformed at a strain rate of $\dot{\varepsilon} = 7000\left[\sec^{-1}\right]$: **(a)** shear band of a failed specimen showing dynamically recrystallized nanograins (arrowed) within region with high dislocation density. The corresponding selected area diffraction pattern (SADP) consists of a ring pattern, which indicates a very fine microstructure. **(b+c)** in the fillet of a SCS deformed to 90% of the failure strain, showing a region deformed mainly by twinning **(b),** an adjacent region **(c)** which exhibits a high dislocation density and DRX (arrowed) but no twins, and **(d)** experimental stress-strain curves for the interrupted mechanical tests on SCS specimens at a strain rate of $\dot{\varepsilon} = 7000\left[\sec^{-1}\right]$.

Figure 2. Calculated averaged volume fraction of DRX and twins in the gauge section, as a function of the averaged plastic strain normalized by the experimentally observed failure strain. Note that twinning precedes by far the onset of dynamic recrystallization.

Figure 3. Local strain rate (normalized by the average specimen strain rate) and evolution of temperature as a function of the normalized averaged plastic strain.

(**a)** The local strain rate is determined over various concentric shells (1 to 3), between *r* and *r*+*dr* ($dr = 0.05[mm]$), with the origin centered on the selected recrystallized element. The strain rate increases markedly as one approaches the recrystallized element, as a clear indication of shear localization and local strain-softening.

(b) Calculated homologous temperatures in the gauge section: A*verage* (solid line), *maximum* local (dashed line), and *average* assuming $\beta = 1$ (dotted line).

Figure 4. Calculated evolution of DRX islands on the outer surfaces of the SCS specimen.

Elements with a DRX volume fraction greater than 5% are marked in red for **(a)** $\varepsilon_p = 0.7\varepsilon_f$ **(b)** $\varepsilon_p = 0.78\varepsilon_f$ **(c)** $\varepsilon_p = 0.85\varepsilon_f$, and $\varepsilon_p = \varepsilon_f$. Note that the band is continuous at the failure strain. Some islands are outlined by dashed lines.

Figure 1

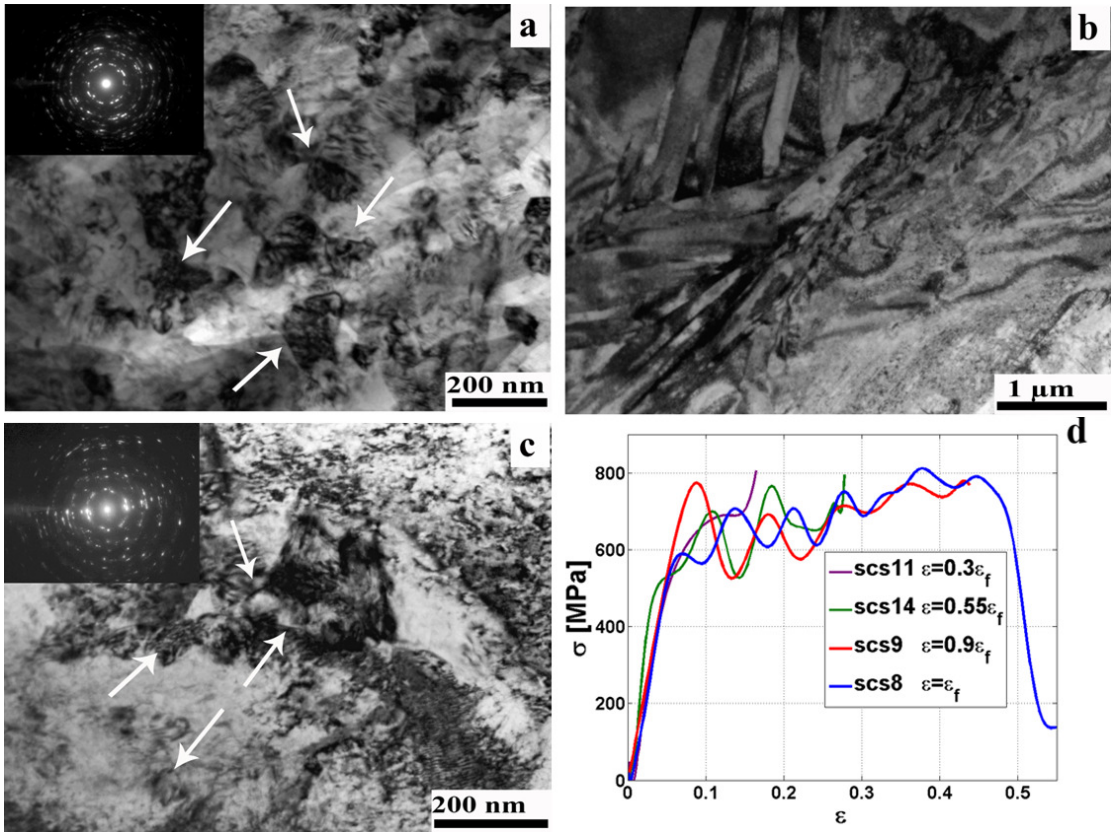

Figure 2

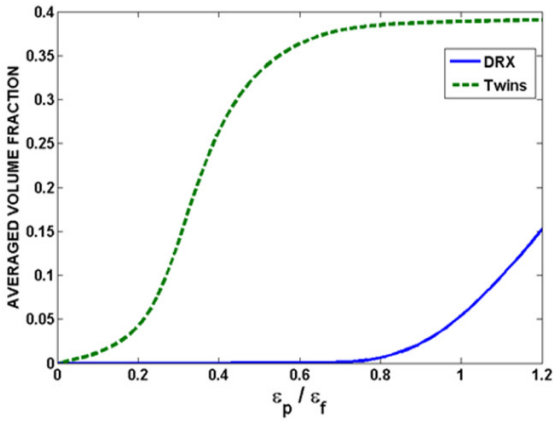

Figure 3

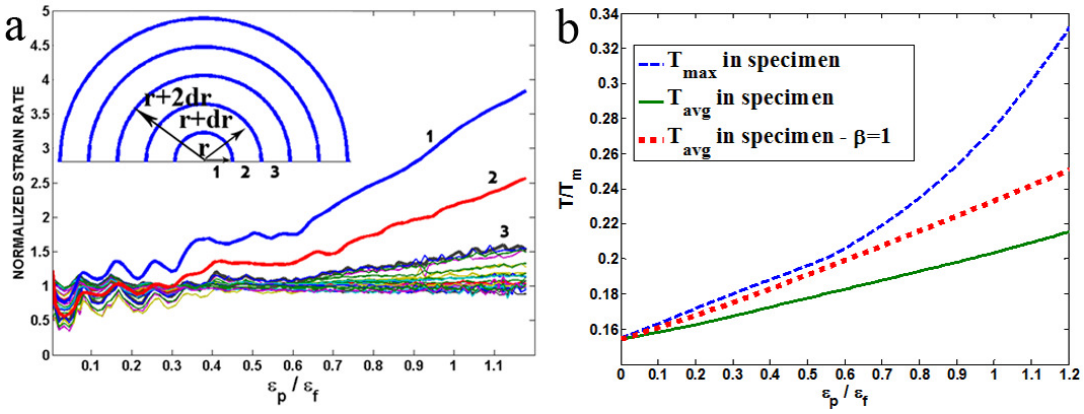

Figure 4